








# The TanDEM-X Mission Phases—Ten Years of Bistatic Acquisition and Formation Planning

Markus Bachmann , Thomas Kraus , Allan Bojarski , Maximilian Schandri, Johannes Böer, Thomas Edmund Busche, José-Luis Bueso-Bello , Christo Grigorov , Ulrich Steinbrecher, Stefan Buckreuss, Gerhard Krieger , *Fellow, IEEE*, and Manfred Zink 

**Abstract**—TanDEM-X is a formation flying interferometer consisting of two SAR satellites. Together they acquire bistatic SAR data of the earth in order to generate a global digital elevation model as well as individual scientific interferometric datasets on user request. This article gives an overview about ten years of acquisition and formation planning for the TanDEM-X mission. This planning on the one hand includes the derivation of the formation, i.e., the 3-D distance between both satellites in orbit. On the other hand, it needs to consider the regions of interest and the mission, satellite, and instrument constraints in order to effectively plan the bistatic acquisitions. During the ten years in operation TanDEM-X successfully completed various mission goals during dedicated mission phases. All these phases, their characteristics as well as the scientific and commercial outcome are described in detail.

**Index Terms**—Acquisition planning, digital elevation model (DEM), formation, global DEM, mission phases, TanDEM-X.

## I. INTRODUCTION

THE TanDEM-X mission is the first bistatic SAR mission with two satellites flying in a close controlled orbit formation [1]. Its primary goal was to deliver a global digital elevation model (DEM) at a 12 m posting with a relative vertical accuracy of 2 m for terrain slopes less than 20% and 4 m for slopes steeper than 20% [2]. The global coverage was acquired between 2010 and 2014 and the final global DEM generation was completed in 2016 [3], [4].

Beyond the global DEM, TanDEM-X offers great scientific potential for both cross-track and along-track interferometry as well as for new radar imaging techniques and applications [5], [6]. Thus, the global DEM phase was followed by a dedicated science phase from 2014 to 2016. In 2016, also acquisitions to prepare the generation of high-resolution DEMs were performed. Between 2017 and 2020, the so-called change DEM, indicating the changes compared to the first global DEM, was acquired. Finally, since mid-2020 an additional science phase has been initiated, which will last until 2022.

Manuscript received September 30, 2020; revised January 27, 2021; accepted February 23, 2021. Date of publication March 12, 2021; date of current version April 7, 2021. (*Corresponding author: Markus Bachmann.*)

The authors are with the Microwaves and Radar Institute, German Aerospace Center, 51147 Köln, Germany (e-mail: markus.bachmann@dlr.de; t.kraus@dlr.de; allan.bojarski@dlr.de; maximilian.schandri@dlr.de; johannes.boer@dlr.de; thomas.busche@dlr.de; jose-luis.bueso-bello@dlr.de; christo.grigorov@dlr.de; ulrich.steinbrecher@dlr.de; stefan.buckreuss@dlr.de; gerhard.krieger@dlr.de; manfred.zink@dlr.de).

Digital Object Identifier 10.1109/JSTARS.2021.3065446

The rest of this article is structured as follows. Section II introduces the relevant theoretical basics in terms of formation flying and DEM accuracy. This is followed by the description of the acquisition planning constraints in Section III. Afterwards, the two TanDEM-X planning systems for planning global coverages as well as individual experimental science acquisitions are described in detail in Section IV. Finally, the Section V provides an exhaustive overview of the different mission phases, their characteristics and results.

## II. MISSION OVERVIEW

This chapter gives a fundamental introduction on the mission and the parameters relevant for the formation and acquisition planning.

The TanDEM-X mission comprises the TerraSAR-X satellite (launched on June 15, 2007) and the almost identical TanDEM-X satellite (launched on June 21, 2010) [2]. Since December 2010, both satellites are flying (with a few exceptional periods only) as a large single-pass bistatic SAR interferometer in a close helix formation at about 514 km of altitude (mean value across the equator). The satellites fly in a sun-synchronous dusk-dawn orbit with 97° inclination and a repeat cycle of eleven days.

### A. Formation Flying

The orbit of the TerraSAR-X satellite is maintained for the entire mission within a 250 m toroidal tube around a predefined reference trajectory [7]. The TanDEM-X satellite orbits on its path around the earth in a helix-like formation relative to the TerraSAR-X satellite with a distance of a few 100 m only, as shown in Fig. 1. This helix formation is realized by carefully maintaining the orbit inclination and eccentricity vectors resulting in a vertical separation at the poles and a horizontal one at the equator [8]. This minimizes the risk of a collision between both satellites even in case of possible system failures and at same time provides suitable baselines for accurate DEM acquisition. The different formations in terms of horizontal and vertical baseline for the whole mission duration are plotted in Fig. 2. The phase of libration is defined as the difference between the relative ascending node and the relative perigee [9]. This means, it determines the rotation direction of the TanDEM-X satellite around the TerraSAR-X satellite as well as the satellite of both, which is crossing the equator first, i.e., the one which has the smaller right ascension of the ascending node. With a

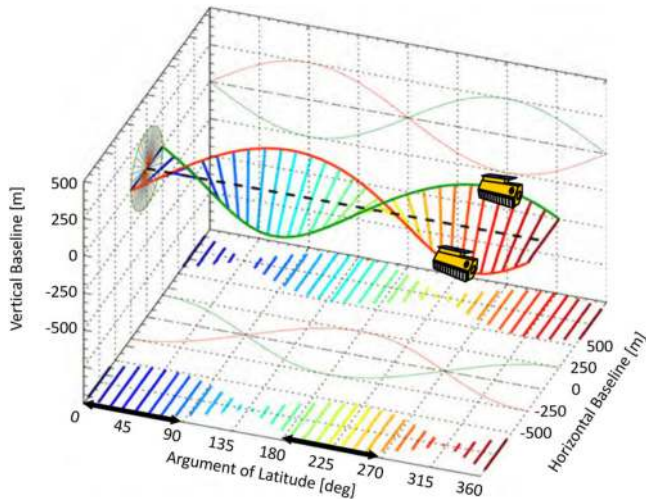


Fig. 1. Illustration of the helix-like formation of the TerraSAR-X and the TanDEM-X satellite over one orbit revolution

phase of libration of about  $0^\circ$  the TanDEM-X satellite seen from behind rotates in clockwise direction around the TerraSAR-X within one orbit; for a phase of libration of  $180^\circ$  the rotation is counter clockwise. The required formation mainly depends on the characteristics of the regions that need to be acquired, the desired incidence angles and the required DEM height accuracy. In Chapter IV, a detailed explanation is given on how these constraints are connected to a consistent acquisition plan.

### B. Height of Ambiguity and DEM Accuracy

The formation is determined by the desired height of ambiguity (HoA), which itself influences the final height accuracy of the DEM. The HoA is defined as the height difference equivalent to a complete  $2\pi$  phase cycle in the interferogram scaled with the perpendicular baseline between both satellites. For the bistatic case, it can be expressed as

$$\text{HoA} = \lambda \cdot r \cdot \sin(\theta_i) / B_\perp \quad (1)$$

where  $\lambda$  is the radar wavelength,  $r$  the slant range,  $\theta_i$  the incidence angle, and  $B_\perp$  the perpendicular baseline. The relative vertical accuracy can, then, be written as

$$\Delta h = \text{HoA} \cdot \Delta\varphi / (2 \cdot \pi) \quad (2)$$

defining  $\Delta\varphi$  as the point-to-point phase error, normally calculated at the 90% confidence interval [10]. According to (2), a lower HoA results in a better relative height accuracy. In contrast to that, DEMs acquired with a low HoA suffer from phase unwrapping problems over terrain with steep slopes, like mountainous regions or degraded coherence over forests, because of volume decorrelation [11]. In order to solve phase unwrapping difficulties, multiple acquisitions with different baselines are combined. In this way, the so-called dual baseline phase unwrapping technique can be used to resolve phase unwrapping errors in the DEM [12]. The approach evaluates the height differences in the phase of two acquisitions over the same terrain and corrects the wrongly unwrapped parts of the scene.

In addition, the two acquisitions can be combined to improve the height performance by reducing the noise like decorrelation [13]. For this purpose, the acquisitions of the second coverage are shifted by half a swath width compared to the first coverage. In this way, the pattern regions with higher antenna gain, i.e., better SNR and, thus, better height accuracy, are combined with lower gain regions at the edges of the pattern main lobe from the other coverage. This results in a rather flat height accuracy distribution across the whole access range, which is not achievable with only one acquisition coverage [14].

Fig. 2, furthermore, shows the resulting height of ambiguity for the acquisitions (yellow diamonds). The dedicated mission phases indicated on the top of the plot are explained in detail in Chapter V as well as the need for the different height of ambiguity values shown here.

## III. PLANNING CONSTRAINTS

### A. Instrument and Satellites Constraints

The TerraSAR-X satellite was originally designed to acquire monostatic SAR acquisitions over dedicated, isolated areas with a multitude of different imaging modes. In contrast to this design, the TanDEM-X mission needs to acquire all land masses of the Earth, i.e., a large area and, hence, a large amount of data. However, due to the initial design goals of the monostatic mission, the bistatic mission is limited by a number of instrument constraints and limited satellite resources imposing challenges to the global acquisition approach.

#### 1) Limited Downlink Capacity

One main restricting factor in each spaceborne SAR system especially for low-earth orbit satellites is the limited downlink capacity. Satellites can only dump data within the visibility range of a ground station unless they are equipped with an optical data link to a geostationary relay satellite [15]. Such relay satellites though were not operationally available at the launch of TanDEM-X. DLR established two own and contracted one external ground station at northern/southern latitudes in Inuvik (Canada), O'Higgins (Antarctica), and Kiruna (Sweden) for dumping the vast amount of TanDEM-X data [16]. In this way, a mean orbit usage, i.e., the mean acquisition time per orbit of 180 s could be realized. However, this equals to only three minutes of acquisition time during one orbit revolution of 95 min. One main goal of the acquisition planning explained in the following chapter is to maximize and homogenize the utilization of the downlink resource as much as possible.

#### 2) Degradation of the Battery

Also, the SAR system itself limits the length of the acquisitions. Even when the solar array of the satellite is completely illuminated by the sun a small portion of battery power is utilized. Moreover, during eclipse times, i.e., when the satellites are in the earth shadow due to their orbit inclination, the power for transmitting the SAR signal is taken from the battery.

This limited the maximal length of data takes at begin of life to about 340 s, depending on the mode and acquisition parameters

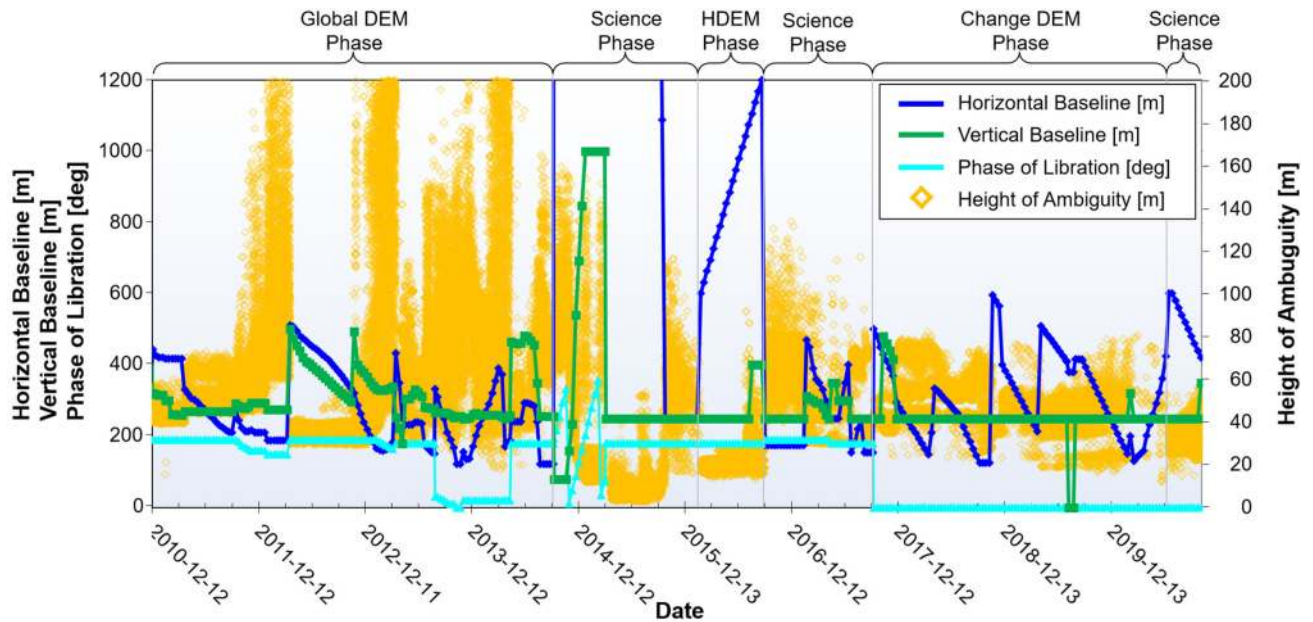


Fig. 2. Formation parameters, i.e., the horizontal and vertical baseline and the phase of libration on the left axis (blue, cyan, and green lines/dots) and the resulting height of ambiguity of the acquisitions on the right axis (golden diamonds). Note, that the formation parameters axis is cut at 1200 m for visual reasons while the maximal values of the horizontal distance increase up to 4.9 km and 3.6 km, respectively, in 2014/2015.

and both due to battery and to respect the thermal limits of the instrument. With the increasing age of the satellites also the battery degradation is progressing. Although the batteries on both satellites are still much fitter than predicted, especially for long data takes their voltages drop more rapidly and to lower values than at begin of life [17], [18]. Hence, since around 2017, the battery is considered as the dominant factor for limiting the acquisition duration restricting the maximal length of data takes.

### 3) Limited Amount of Propellant

Both satellites host a tank retaining 74 kg of hydrazine. In addition, the TanDEM-X satellite also accommodates a cold-gas system for formation keeping. Orbit keeping and formation changes and maintenance continuously consume propellant and limit the lifetime of the satellites. Cold gas is already almost emptied since 2016. In order to ensure a long mission duration, measures to efficiently utilize the propellant while at the same time ensuring appropriate baselines need to be considered in the planning process. This is mainly considered by only slowly changing the satellite formation or by utilizing orbit inclinations slightly different for each satellite to establish a continuously drifting formation change.

## B. Mission Constraints

1) *Joint TerraSAR-X/TanDEM-X Mission*: The main purpose of the TerraSAR-X mission is to deliver monostatic SAR images for scientific and commercial customers [19]. With the TanDEM-X satellite launched in 2010, both satellites share the acquisition of monostatic TerraSAR-X data takes. In addition, the TanDEM-X mission exploits the bistatic capabilities of the system. As the TanDEM-X mission was designed as an add-on

to the TerraSAR-X mission, also a joint mission concept was developed for satellite resource sharing. This joint mission approach foresees a coexistence of both missions. One important aspect in this approach is the TanDEM-X acquisition plan. This acquisition plan is derived well in advance before the first acquisition is carried out and for a long time frame. It is published and made available to the scientific and commercial user coordinators. This allows the TerraSAR-X users to detect conflicts in advance and preferably plan around the TanDEM-X acquisitions. The TanDEM-X acquisition planning also tries to avoid acquisitions in consecutive cycles at the same orbit position, thus allowing the TerraSAR-X mission to acquire at least every second cycle [20].

2) *Commercial User Conflicts*: The TanDEM-X mission (and also the TerraSAR-X mission) is realized in a public-private partnership between the German Aerospace Center (DLR) and Airbus Defence and Space (Airbus D&S). While DLR is responsible for the scientific utilization of the system, Airbus exploits the commercial potentials of the mission serving external customers with SAR and DEM data.

One important commercial field for the exploitation of SAR images are stacks for urban or economic planning. As the TanDEM-X mission needs to cover all land masses of the earth, conflicts between commercial customers and TanDEM-X acquisitions are inevitable. A priority system was established in order to manage these conflicts. Each TanDEM-X acquisition needs to be acquired within a certain height of ambiguity range. The formation is rather stable or only slowly changing. Hence, during acquisition calculation an estimation is provided for how many cycles an acquisition can be postponed until the height of ambiguity becomes unsuitable. In this way, most of the potential conflicts can be solved by shifting the conflicting TanDEM-X



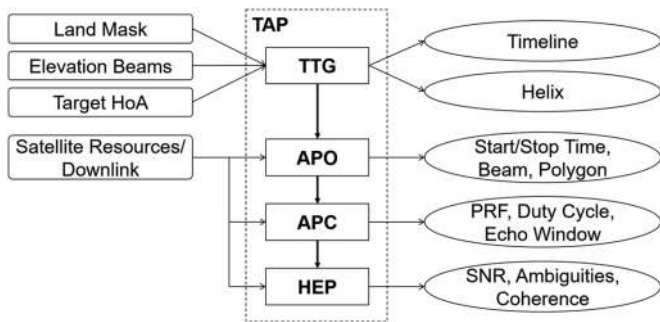


Fig. 3. Block diagram of the TAP containing the main modules TTG, APO, APC, and HEP.

data takes automatically for one cycle. Finally, due to a flexible replanning tool, it is even possible to solve almost all residual conflicts by shifting the TanDEM-X data takes manually.

Hence, an intelligent planning concept is needed to optimally exploit the satellite resources and mission constraints.

#### IV. TANDEM-X ACQUISITION PLANNING SYSTEM

The nominal monostatic SAR image acquisition (TerraSAR-X mission) as well as the derivation of the global DEM (TanDEM-X mission) share the same satellite resources. Therefore, a joint acquisition concept has been elaborated in order to ensure both missions goals. TanDEM-X DEM data takes are planned in the so-called DEM acquisition timeline. In order to fulfill the requirements of the height accuracy of the DEM, the formation is optimized accordingly with respect to each region that has to be mapped, since the HoA is changing with beam and latitude.

The planning system described below is a set of software tools particularly developed for the TanDEM-X mission. Thus, all the characteristics of the mission could be thoroughly considered to allow a reliable planning and an efficient utilization of the resources of the satellites and the mission. The planning system consists of two main components. The TanDEM-X acquisition planner (TAP) on the one hand is used to plan the large global coverages. The system command generator framework on the other side plans scientific and experimental acquisitions and data stacks.

##### A. Coverages: TAP

The TAP [21] system is divided into four modules, which are shown in the diagram in Fig. 3. The functions and outputs of the modules are described as follows.

- 1) Coarse planning with iterative formation and orbit usage optimization

The first step of the planning is a coarse derivation of an acquisition timeline for a given time frame, e.g., for one year. Its goal is to find a formation, which optimally distributes the required acquisitions, i.e., which maximizes the orbit usage while at the same reduces the required formation changes.

This step is performed by the TanDEM-X timeline generator (TTG). The acquisition timeline derivation starts with the

evaluation of the area to be acquired. It calculates from which orbital position and with which beam an area of interest has to be mapped. The main inputs are a mask of the area, which needs to be acquired (LandMask), the available elevation beams, and the target HoA. The acquisition strategy is constrained by the following factors.

- 1) Radar geometry with look angles and beam information (each beam overlaps with the adjacent one by 4 km).
- 2) *Mapping strategy*: the nominal strategy is to record data during ascending orbits in the northern hemisphere and during descending orbits in the southern one. The reason for this strategy is the helix formation with orbit regions (quarters) with large baselines suitable for interferometric imaging and orbits pieces with small baselines degrading the height accuracy [20].

Due to the fact that the distance between two adjacent ground projected tracks is decreasing with increasing latitude, a smaller number of swaths is required with increasing latitude to cover a similar area on ground.

- 1) *Target HoA*: it is derived to reach a compromise between small height errors and robust phase unwrapping.
- 2) *Satellite resources*: power and thermal resources of the satellites limit the acquisitions. A mean acquisition time of 180 s per orbit is considered at begin of life.
- 3) *Ground station network and downlink capacity*: the network used for the downlink of the TanDEM-X mission includes the ground stations in Inuvik, O'Higgins, and Kiruna [16].
- 4) *Formation flying limitations*: The vertical and horizontal baselines need to stay within a certain limit. The lower limit is given by safety reasons, the upper one by instrument reasons like satellite synchronization [22]. In addition, the increase of baselines per cycle needs to be minimized in order to conserve the limited resource propellant.

Once the area to be acquired is determined, the calculation of formation parameters that define the helix, i.e., the vertical and horizontal distance, is performed for each repeat cycle of eleven days. Based on these assumptions and constraints, the timeline is derived iteratively. This iterative process changes the formation parameters and optimized the distribution of the acquisitions and the orbit usage as explained previously. The process can run automatically for homogeneous acquisition scenarios as applied in the first global DEM acquisition phase (cf., Section V-B). Or it can be executed semimanually in case of many different regions like for the change DEM (cf., Section V-F).

The resulting timeline includes all the bistatic data takes (TAPTakes) to be acquired with their start/stop times.

- 2) Detailed planning

After the coarse timeline planning the exact parameters of the each resulting data take is calculated. Only in this way, it is possible to precisely determine the satellite resources consumed by each data take. One of these resources is the payload data volume, which is different for each data take. It depends on instrument parameters like pulse repetition frequency (PRF), the used bandwidth and the rate of the block adaptive quantization (BAQ), which are set based on, e.g., the underlying terrain or the

backscatter of the scene on ground. With these exact parameters a further optimization is performed in order to utilize the downlink capacity as optimal as possible.

The determined TAPTake start and stop times, together with the elevation beam for each data take are, thus, forwarded to the acquisition parameter optimizer (APO), which extends these times by adding margins for warm-up and calibration sequences of the instrument.

From these extended start and stop times, the acquisition parameter calculator (APC) derives a detailed set of acquisition parameters (APSets) representing the relevant instrument parameters. The set includes information like the echo window position and length, the PRF, and the receiver gain setting. In addition, it contains data concerning the active and the passive satellite and their memory and energy consumption. Furthermore, also alternative parameters for the transmit duty cycle, the data rate compression factors and the receive bandwidths are stored in form of different proposals. Consequently, these proposals have different memory and energy consumptions. The best proposal will be selected by the APO later on while scheduling the available satellite resources.

For each single proposal in the APSet, the height error predictor (HEP) estimates the height performance. First, the total coherence and ambiguity values are evaluated. From these results, the relative height error is derived according to (2). These quantities give an estimation of the expected interferometric performance.

In the last step of the acquisition timeline generation, these sets of parameters are optimized by the APO. The APO selects the best acquisition parameters and height error sets for each TAPTake in order to obtain a timeline with a homogeneous and high height accuracy.

During most of the TanDEM-X mission phases, the available downlink capacity was the major limiting factor. The on-board solid-state mass memory keeps already acquired acquisitions in memory until the next ground station is in visibility. The storage capacity of TanDEM-X is 768 GBit since begin of life, while that of TerraSAR-X is 384 GBit. Therefore, the mass memory of the latter must be dumped first. Further details can be found in [20] and [21]. Also, this constraint is reflected in the operational acquisition planning in order to facilitate an optimized usage of all available resources.

Finally, several further products are derived from the final formation and acquisitions: From the formation parameters, the TanDEM-X satellite's reference orbits are generated. In addition, the exclusion zones are calculated in order to ensure safe formation flight [2]. The planned acquisitions are forwarded in form of TanDEM-X orders to the TerraSAR-X/TanDEM-X mission planning system [23]. The mission planning system combines the TanDEM-X acquisitions with the TerraSAR-X data takes into a consistent mission timeline and performs its uplink for execution on the satellite.

### B. Time Series, Stacks, and Special Data Takes: System Command Generator

The TAP as explained previously is the tool of choice to plan of large coverages. For planning of individual scientific

acquisitions with special modes or commanding parameters or for planning acquisition time series (data stacks) the so-called system command generator (SCG) is used. The main interface for the SCG is a table with the desired acquisition geometry and dedicated parameters like the imaging mode and the polarization settings. These parameters are provided by the TanDEM-X science coordinators derived from the requests of scientific users, which they submitted via the TanDEM-X science server [24]. The input parameters can be manually adapted for experimental and scientific data takes with special demands on modes or instrument commanding (see below and Section V-C).

The SCG also utilizes tools from the TAP like the APC. Hence, all data takes are generated from a common, verified system, which ensures identical acquisition results.

The SCG is used to regularly plan the following acquisitions.

#### 1) Long-term system monitoring data takes

The TanDEM-X mission runs very reliable and stable. In order to ensure this stability of the mission, it is necessary to continuously monitor the system. Therefore, dedicated data takes are planned, acquired, and evaluated on a regular base, e.g., every first, second, or third cycle. One example for these data takes are the baseline calibration data takes used to monitor the stability of the baseline between the satellites [25].

#### 1) Super test sites

More than 60 super test sites are continuously acquired and monitored. These super test sites include among others glaciers, volcanoes, and forest areas. The super test sites are of big interest for the science community. Thus, sometimes the acquisitions over these sites stand in conflict to other scientific acquisitions. In this case, a semimanual approach is performed in order to achieve an optimal utilization of the system in these areas.

#### 2) Special commanding

The SAR instruments on both satellites host a very flexible commanding system, which makes possible to command experimental acquisitions with high demanding time or instrument constraints. Hence, very exotic data takes can be planned on special user request. Therefore, the command set, which is used to set the individual instrument parameters on board the satellite can be adapted by hand. This was used for experiments like, e.g. Staring spotlight acquisitions (before their operational implementation) [26], for bidirectional acquisitions [27] or for so-called aperture switching data takes for ocean current measurements [28].

After the planning process, the data are acquired and dumped via the ground station network. It is then sent to the processing facility at the earth observation center, Oberpfaffenhofen, Germany. Being processed by the operational Integrated TanDEM-X Processor [29], the data are finally available and can be accessed via the EOWEB GeoPortal [30] for scientific use.

## V. MISSION PHASES

This Section explains different phases of the TanDEM-X mission, which are summarized in Fig. 4.

### A. Commissioning Phase

The commissioning phase of TanDEM-X lasted for about six months [31]. With the launch of the TanDEM-X satellite on June

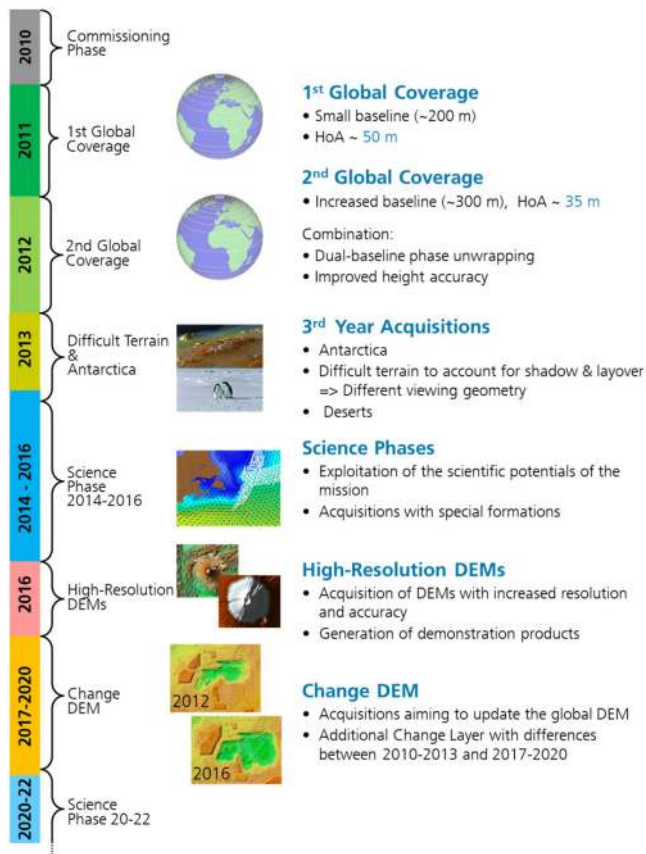


Fig. 4. TanDEM-X mission phases timeline

21, 2010, the launch and early orbit phase started for checking out the satellite systems and activating the SAR instrument. Within one month the TanDEM-X satellite was flown towards the TerraSAR-X satellite and stopped in a distance of 20 km behind TerraSAR-X. During the next three months, the TanDEM-X satellite was monostatically calibrated and prepared for the formation flight [32], [33]. On October 14, 2010, the TanDEM-X satellite entered the close formation with TerraSAR-X with a horizontal baseline of about 360 m. Until December 12, 2010, the bistatic capabilities of the system were checked out, verified, and calibrated in order to start the acquisition of the global DEM [34]. Finally, even during the next two years the processing system was adjusted and calibrated while already acquiring the global DEM [35], [36], [37].

### B. Global DEM Acquisition Phase

In the first two years of operations two global coverages of the complete earth's land masses, excluding Antarctica, were acquired. All the acquisitions were carried out in nominal right-looking observation mode. In order to perform the acquisitions with suitable baselines the orbit parts in which the acquisitions were executed are ascending orbits in the northern hemisphere and descending orbits in the southern hemisphere. The nominal acquisition mode for the DEM generation is the stripmap mode

in single (horizontal) polarization. This mode is a good compromise between achievable resolution in the order of 3 m for SAR products and a swath width in the order of 30 km that allows us a coverage at the equator with nine consecutive beams and, hence, in a defined time. The used receive bandwidth is 100 MHz or 150 MHz acquired with a BAQ of 8:4 or 8:3 in order to restrict the amount of data acquired

The acquisition of the first global coverage was finished in March 2012. In this first year, the target HoA was set to 50 m or 60 m, respectively (compare Fig. 2). Since the HoA depends on the incidence angle and the helix (changing with the latitude), the formation, in terms of horizontal and vertical distance between the satellites, was changed accordingly to keep a stable HoA, as close as possible to the target HoA. This can be observed in Fig. 2, where the formation parameters are adapted along the mission time; the vertical and the horizontal distances decrease progressively during the two global acquisitions for first and second year, respectively. It can be recognized that within the two main acquisition phases, the helix has been slightly reconfigured several times in order to achieve different target HoAs [38]. An explicit example can be seen in April 2011, where the minimal HoA was reset from 40 m to 45 m in order to deal with the strong volume decorrelation over tropical forests.

In order to allow reliable phase unwrapping, additional acquisitions were performed over the rain forest in south eastern Asia and over mountainous regions. This included acquisitions with even higher HoA in the order of 60 m to 80 m, which require very small baselines. This is visible in Fig. 2, starting from October 2011, when the variation of the HoA increases.

In March 2012, the acquisitions of the second global coverage started lasting until April 2013. According to the acquisition strategy the target for the HoA was reduced from 50 m to 35 m in this second coverage [1]. The decrease of the HoA by a factor of 0.7 has been found to be optimal in order to combine the two coverages to resolve phase unwrapping errors and to improve the relative height error [39]. In Fig. 2, the transition from the first to the second year is clearly visible as the sudden jump of the formation and a consequent decrease of the HoA.

The third and fourth acquisition year in 2013 and early 2014 was dedicated to difficult terrain and Antarctica.

Difficult terrain in form of mountainous regions suffers from shadow and layover effects due to the side-looking geometry of the SAR system. In order to mitigate these effects, mountains were additionally acquired from the opposite viewing geometry, i.e., on the northern hemisphere in descending orbits instead the nominal ascending orbits. Therefore, the rotation direction of the TanDEM-X satellite in the helix was swapped in order to obtain appropriate baselines [40]. This can be seen in Fig. 2, where the phase of libration (cyan) changes from about  $180^\circ$  to  $0^\circ$ .

Also, sandy deserts are considered as difficult terrain for SAR systems as dry sand has a very low backscatter under nominal incidence angles. In order to increase the signal-to-noise ratio all sandy deserts have been reacquired with very steep incidence angles. Due to the shorter distance to earth and the reduced incidence angle, leading to stronger backscatter characteristics,



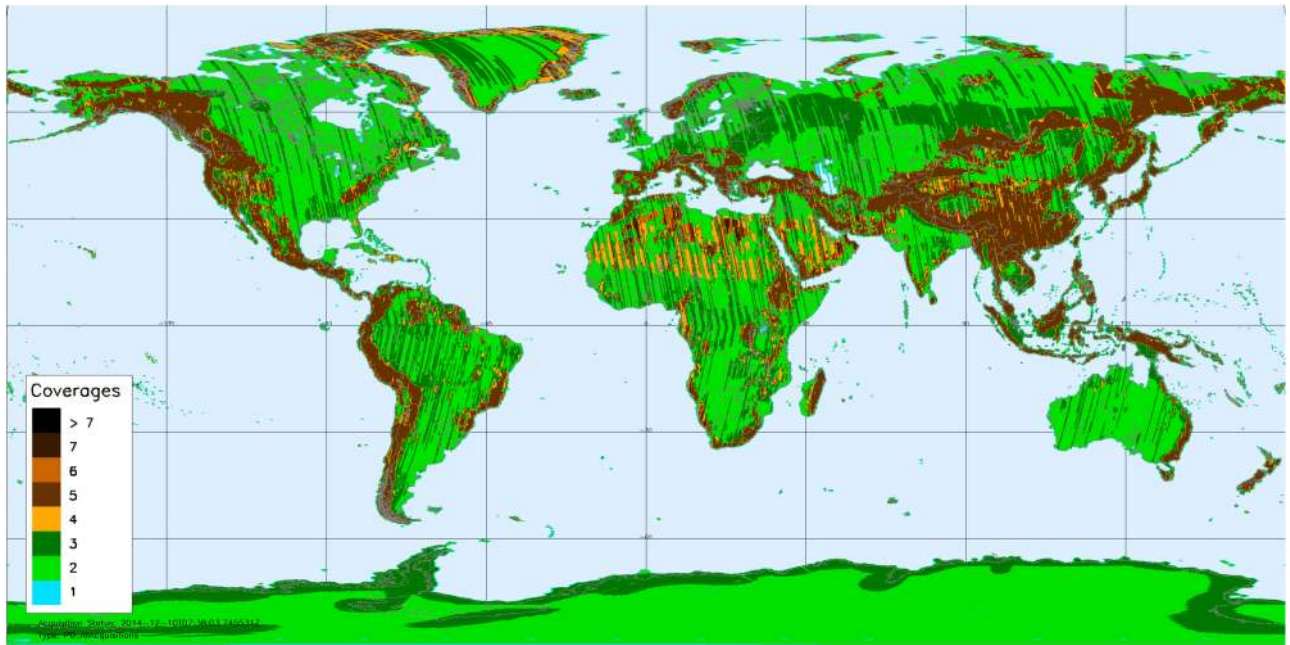


Fig. 5. Acquired number of coverages for the global DEM acquisition between 2010 and 2014. In general, at least two coverages have been acquired. In regions with difficult mountainous terrain even up to eight acquisitions have been performed.

a higher receive signal level is achieved and hence the height performance is improved significantly [41].

Finally, Antarctica was acquired during local winter times as the backscatter of ice areas during melting periods contradicts a good DEM accuracy. Especially for the inner regions of Antarctica, left-looking acquisitions had to be exploited and a very flat beam with  $60^\circ$  of incidence angle was used to reach the South Pole. This acquisition of Antarctica is one of the main advantages compared to the widely known shuttle radar topography mission DEM [42], which is limited to areas within  $\pm 60^\circ$  latitude.

In total, 68 500 global DEM acquisitions have been performed during the first seven years of TanDEM-X mission. Fig. 5 shows the number of coverages acquired for the global DEM. At least two coverages have been acquired over all land masses on earth. In some regions, especially over difficult terrain like in mountainous areas, the performed acquisitions sum up to even seven coverages.

The resulting global DEM product shows an unprecedented accuracy for a global product. The main parameters describing the DEM accuracy are the relative and the absolute vertical accuracy.

The absolute vertical accuracy represents the uncertainty in the height of a point with respect to the WGS84 ellipsoid caused by uncorrected, slow-changing systematic error. It was assessed using ICESat measurement data as reference values [43]. All 19 389 DEM tiles ( $1^\circ \times 1^\circ$  DEM cell) were evaluated. The evaluation shows an absolute height accuracy at 90% confidence level of 3.49 m [44]. This is well below the 10 m mission specification [1], [4]. Highly vegetated areas and ice or snow-covered regions drive this error due to their strong volume decorrelation effects. The corresponding absolute height accuracy over forest tiles hence is only 2.33 m. Over ice, also due to different penetration

depths between the TanDEM-X radar and the ICESat Lidar sensor, it is 6.37 m. Excluding these areas results in an improved absolute height accuracy of only 0.88 m for the remaining 12 257 tiles.

The vertical height accuracy describes the accuracy of the DEM in terms of local height differences and accounts for random errors [45]. The mission specification states a relative height error of 2 m for flat and 4 m for steep terrain with slopes larger than 20% at 90% confidence level. This specification is met for 97.76% of all tiles again excluding tiles, which are mainly covered by ice/snow or densely vegetated forest affected by strong volume decorrelation phenomena [46]. A more detailed description of the results can also be found in [4].

### C. Phase-Independent Scientific Planning

During the whole TanDEM-X mission duration, science data takes have been acquired over super test sites or on scientists' request. An overview of these acquisitions is shown in Fig. 6. Although the amount of acquisition sites seems rather small compared to the global DEM coverages, about 60 800 science acquisitions have successfully been planned and acquired throughout the mission duration. This is almost the same number than for global DEM acquisition, though most of the science acquisitions are much shorter than the long global DEM acquisition stripes.

The global DEM was only acquired in single polarization stripmap mode. In contrast to that, the scientific acquisitions use almost the full spectrum of modes and beams (except the ScanSAR mode). This spectrum includes, e.g., acquisitions in stripmap and spotlight mode, in nominal and extended performance incidence angle range, right and left looking, and single and dual pol mode [47].

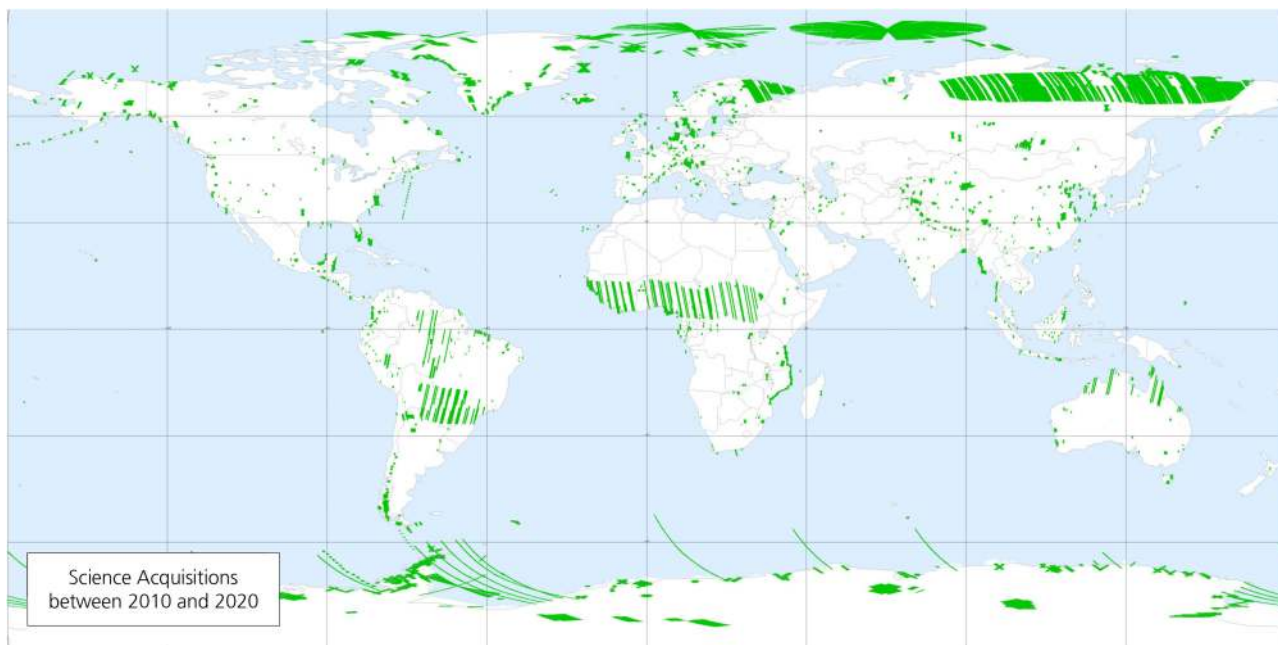


Fig. 6. Map of science acquisitions on super test sites and with dedicatedly commanded data takes for scientific purposes in the time frame from 2010 to 2020 but excluding the dedicated large scientific coverages explained in Sections V-C–V-G.

Besides the nominal requests that are considered in the mission timeline, even dedicated special campaigns could be performed. Some examples of these campaigns are as follows.

- 1) The measurement of sea surface currents is only possible if the satellites are less than about 50 m apart in flight direction. In the nominal geometry, this is only the case near the poles, when one satellite overtakes the other. For dedicated ocean current measurement campaigns, an along-track shift was established such that short along-track baselines were realized at mid-latitudes [48].
- 2) For a campaign to measure the sea-ice drift in Antarctica, a joint airborne, and TanDEM-X measurement campaign was carried out. Coordinated acquisitions allowed the quasi simultaneous space and airborne measurements of large areas in the Weddell sea [49].
- 3) The measurement of ocean and atmospheric parameters was enabled by a joint acquisitions campaign between TanDEM-X and aircrafts in the Caribbean sea within the context of the Harmony proposal for ESA's earth explorer 10 call [50].

#### D. Science Phase 2014–2016

Since 2014, dedicated phases concentrating on formations for the scientific purpose have been flown. The science phase from 2014 to 2016 can be separated into three subphases, as shown in Fig. 7. The pursuit monostatic phase, which lasted for seven months; the large horizontal baseline phase with a duration of about six months; and the forest phase of another six months.

1) *Pursuit Monostatic Phase*: The main purpose of the pursuit monostatic phase was to enable acquisitions with larger baselines of approximately 1 km for areas at northern latitudes.

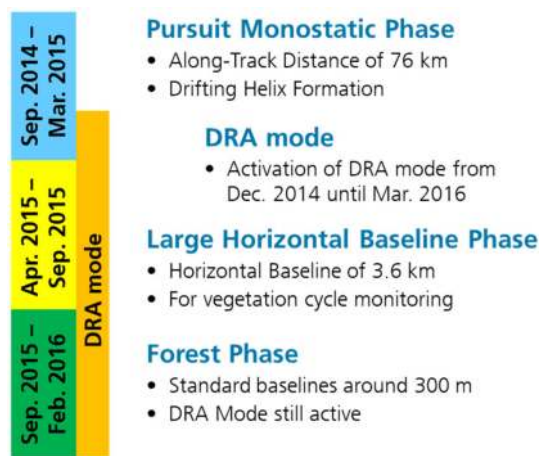


Fig. 7. Science phase timeline.

During the nominal DEM acquisition, the vertical baseline at the poles is in the order of 250 m. A very large vertical baseline would require a very higher amount of propellant for maintaining the helix formation. In addition, the along-track baseline in the helix is twice the vertical baseline and, thus, would also be very large. Such large along-track distances would lead to a loss of correlation for the bistatic acquisitions. Thus, the pursuit monostatic phase was designed to mitigate these constraints. By releasing the close formation, it is possible to disable the compensation of the eccentricity drift. This leads to a drifting helix and, hence, to large horizontal baselines also at high latitudes. This, however, allows us to perform monostatic acquisitions only. As they were coordinated to ensure the same instrument



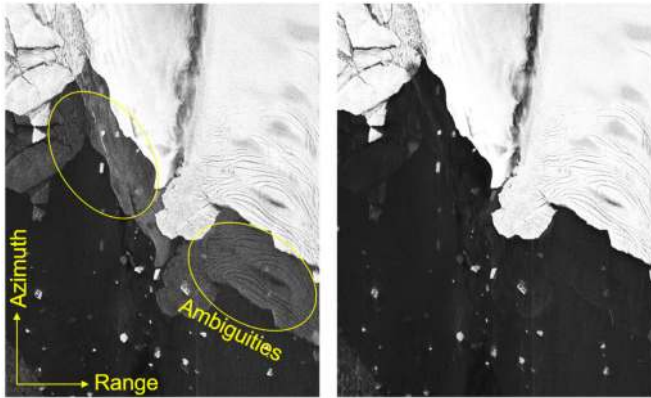


Fig. 8. Azimuth ambiguity reduction by exploiting the multiple phase centers demonstrated over a glacier in Antarctica. The left image shows the ambiguity of the ice shelf in water. In the right image, the ambiguity is almost no longer visible.

parameters, they can be processed like repeat-pass acquisition with a very small temporal gap. For areas with stable ground and low temporal changes DEMs could be generated.

An along-track distance of 76 km (which equals ten seconds) is the minimal distance to avoid SAR interferences in case of staring spotlight acquisitions. In staring spotlight both satellites illuminate the same point on ground and the data takes last for up to ten seconds. A larger distance, however, is critical as a horizontal distance needs to be established in order to compensate the earth rotation allowing acquisitions with the same ground track. For an along-track distance of ten seconds a horizontal baseline of already 4.9 km is required. A large amount of propellant is required to establish this large baseline. The pursuit monostatic formation was entered in September 2014. Close formation was re-established in February 2015 with the start of the large horizontal baseline phase.

Prominent examples for the exploitation of the pursuit monostatic formation are the mapping of sea ice drifts [51] or oil spill detection [52]. A general examination can be found in [53].

2) *DRA Mode*: Another feature of the TerraSAR-X and TanDEM-X satellites is the dual receive antenna (DRA) mode, which allows the acquisition of quad-polarization and pairs of along-track interferometry data takes. In this mode, the antenna is split into two parts in flight direction. The redundant receiving chain is activated in order to receive radar data via a second independent channel, which allows us to acquire with two phase centers separated in azimuth. As both, the primary and the redundant chain are used, this mode is only enabled during dedicated campaigns to minimize the risk of losing one or both chains.

The DRA mode is especially interesting for ocean or sea surface measurements, as described in [54]. The combination between DRA mode and pursuit monostatic formation can also be used for ship velocity estimation [55]. An overview on the performance of the DRA mode is given in [56]. Also, instrument-related experiments with the DRA mode have been performed, for example to reduce azimuth ambiguities [57], [58]. This

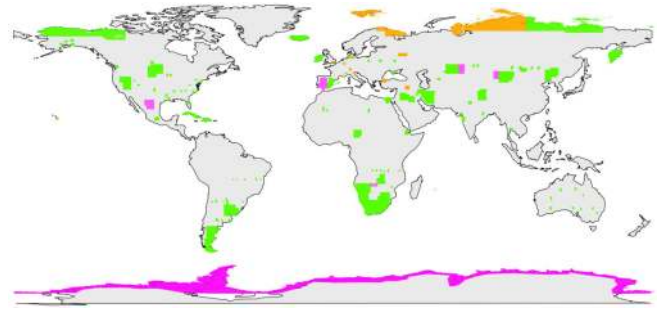


Fig. 9. Test areas that have been acquired during the large horizontal baseline phase over permafrost areas and to assess DEMs acquired with very large baselines. The different color indicate different acquisition periods between during 2015.

example can be seen in Fig. 8, where a reconstruction algorithm uses two or even four (DRA on both satellites) channels and, hence, phase centers in order to reduce ambiguities and consequently increase timing flexibility.

3) *Large Horizontal Baselines Phase*: One main purpose for a large horizontal baseline phase in 2015 was the acquisition of a full growing cycle of crops and other agricultural vegetation on the northern hemisphere. Therefore, the phase lasted from April, when the vegetation starts to grow until late September, when the harvest is taken. The horizontal baseline in this phase was increased to 3.6 km at the equator. For mid-latitudes the baseline was still in the order of 1.5 to 2 km. Even short vegetation like rice could be accurately monitored with this formation [59] as well as it enabled the determination of different crop parameters [60].

In addition to the acquisition on scientific user request larger areas over permafrost and sites to demonstrate DEMs with very high height accuracy were acquired. Finally, also the outer regions of Antarctica were acquired in local winter season. These larger test areas are shown in Fig. 9.

4) *Forest and Arctic Phase*: The large horizontal phase was followed by a phase with formations in the nominal range of a few hundred meters but with emphasis on forest areas. As the DRA mode was still activated, full-polarimetric interferometric images of forest areas, especially boreal forest and tropical forest were acquired with different baselines.

This first Forest and Arctic Phase was followed by the high-resolution DEM (HDEM) preparation phase (see following section). After this phase, a second Forest and Arctic Phase was executed between September 2016 and September 2017. During this period, again forests, permafrost areas, and the outer regions of Antarctica and Greenland were acquired to monitor temporal changes.

#### E. HDEM Preparation Phase 2016

One of the secondary goals of the TanDEM-X mission was the derivation of so-called high-resolution DEMs. These DEMs are specified with much more stringent height requirements and were originally derived from the HRTI-4 specification. The

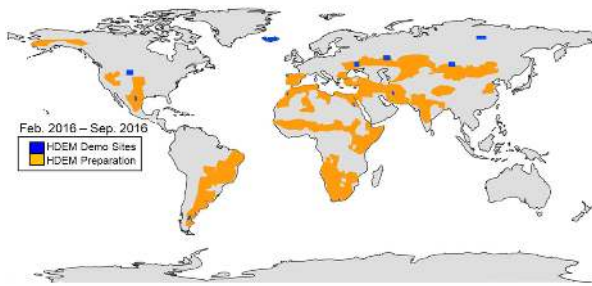


Fig. 10. Areas that have been acquired in 2016 for the demonstration and preparation of HDEMs.

horizontal resolution requirement was  $6\text{ m} \times 6\text{ m}$  with a relative height accuracy better than  $0.8\text{ m}$  [61].

To achieve such high accuracies, the height of ambiguity has to be small, which requires large baselines. However, with small heights of ambiguity, it is not suitable to acquire areas with high vegetation like forests which would suffer from decorrelation in X-band [11]. In addition, a combination of three to four acquisitions is necessary to achieve the height accuracy. Also mountains cannot be acquired properly due to large phase unwrapping problems. Mostly rather flat areas with lower vegetation were selected for the demonstration of HDEMs, which is shown by the blue areas in Fig. 10. These were acquired several times to learn about HDEM acquisition and processing. The acquisitions shown in orange were acquired once in order to prepare for larger HDEM coverages. However, both the commercial as well as the scientific interest was not as expected and finally the acquisition of large HDEM coverages was dropped. Instead the so-called change DEM, a new mission product on global scale was introduced.

#### F. Change DEM Phase 2017–2020

The global DEM generated until 2016 was successfully utilized by the commercial partner (Airbus D&S). Great scientific interest was raised with the scientific release of the DEM data in late 2017 as well. However, a part of the data used for DEM generation was already more than seven years old when the DEM was released. A lot of changes in the topography of the earth took place during this time. Additionally, the satellites were still in good shape and there were sufficient consumables for several more years of operation left [62]. Thus, the mission decided to acquire a further global coverage in order to update the first global DEM in form of a self-contained change DEM product.

1) *Lessons Learned:* During the processing of the global TanDEM-X DEM, the team gained much experience with the acquisition of different types of land cover and terrain and the exploitation of the system. Also, a number of disadvantages of the used acquisition strategy were faced. Many of these disadvantages could be reverted by dedicated additional acquisitions. The following list shows some of the lessons learned.

- 1) Data for DEMs over glaciers or snow-rich mountains explicitly need to be acquired during local winter time, as melting ice or snow shows a very bad SNR performance during summer time.

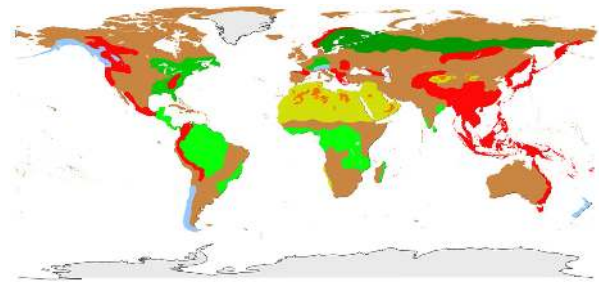


Fig. 11. Different land types for the change DEM acquisition between 2017 and 2020 with the colors describing the dominant land types given as follows: blue: glaciers, green: forests, red: mountainous forested areas, yellow, and orange: deserts, brown: rest of the world. A more detailed explanation including the acquisition constraints is given in Table I.

- 2) The baseline and the corresponding height of ambiguity (HoA) needs to be different for different land cover types and should be in a well-defined range.
  - Glaciers, mountains, or mountainous forests need be acquired with HoAs between  $45\text{ m}$  and  $90\text{ m}$ .
  - Tropical forests can be acquired year-round. However, due to high but varying trees, the HoA needs to be larger than  $50\text{ m}$ .
  - Sandy deserts need to be acquired with very steep incidence angles to overcome the low backscatter of sand and hence to increase the low signal-to-noise ratio.
  - Urban areas would profit from the acquisition with different multiple baseline and opposite view geometries. The acquisition of cities with multiple baseline is one main topic of the Science Phase 2020–2022 (see Section V-F).
  - The remaining areas of the world show mainly bare soil and rock or short vegetation. They can be acquired with a lower height of ambiguity in the order of  $30\text{ m}$  to  $35\text{ m}$ . Thus, only one coverage is sufficient to achieve a fair height accuracy.

For this purpose and considering the lessons learned mentioned above, the earth was separated into dedicated large-scale acquisition areas for the change DEM acquisition plan according to the dominant land classes and terrain types, as shown in Fig. 11. For each acquisition area certain acquisition constraints listed in Table I and indicated by the same color as in Fig. 11 need to be observed.

In addition, several aspects have been identified, which could be considered for follow-on missions, such like Tandem-L [63].

- The low orbit usage of the TanDEM-X system leads to a long duration of about one year to acquire one global coverage. Future systems with longer acquisition time per orbit could realize a higher temporal coverage in the order of month or weeks in order to improve the temporal sampling of the data.
- The optimal spatial resolution depends on the main purpose of the measurement or image. For forest studies, a reduced spatial resolution seems acceptable. For accurate DEMs over urban areas, the spatial resolution should be at least in the order of the TanDEM-X DEM in order to resolve fine structures or changes.



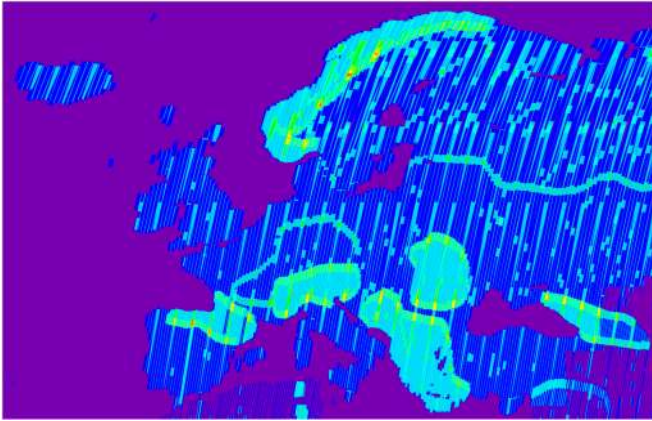


Fig. 12. Acquisitions over Europe (Blue: one acquisition, cyan: two acquisitions, green/yellow/orange: three or more acquisitions).

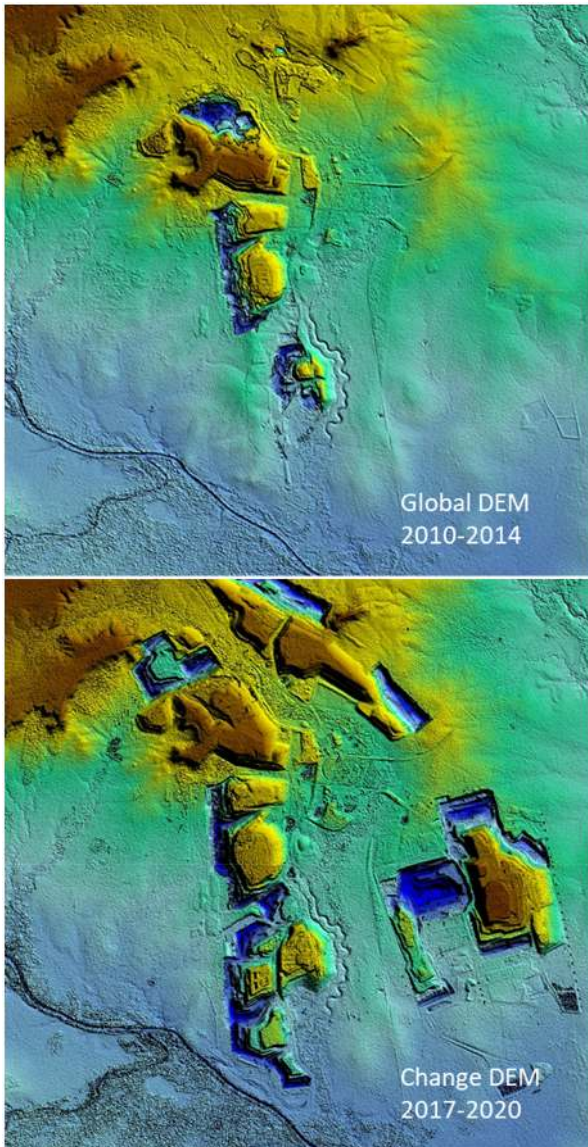


Fig. 13. Example of the change DEM comparing the changes in a mining area in eastern Australia from 2012 to 2018.

TABLE I  
ACQUISITION PARAMETERS FOR THE CHANGE DEM PRODUCT

Region	Coverages	Season	Height of Ambiguity	Inc. Angle Range
Mountains with Forest	2	Local summer	55 - 75 m (1 <sup>st</sup> ) 45 - 53 m (2 <sup>nd</sup> )	27 - 49 deg
Glaciers	2	Local winter	55 - 75 m (1 <sup>st</sup> ) 45 - 53 m (2 <sup>nd</sup> )	29 - 47 deg
Tropical forest	1	Year round	50 - 60 m	27 - 49 deg
Temperate & boreal forest	1	Local summer	50 - 55 m	27 - 49 deg
Deserts with Mountains	2	Year round	55 - 75 m (1 <sup>st</sup> ) 45 - 55 m (2 <sup>nd</sup> )	27 - 49 deg
Deserts	1	Year round	23 - 45 m	14 - 38 deg
Permafrost area	1	Local winter	35 - 45 m	29 - 47 deg
Rest of the world	1	Year round	35 - 45 m	27 - 49 deg

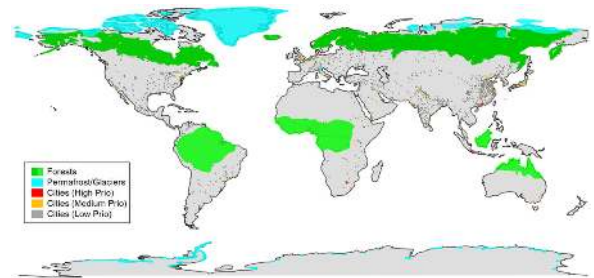


Fig. 14. Areas acquired during the science phase 2020–2022. The main focus of this science phase is on forested areas, on permafrost regions and on urban areas.

- The wave length in X-band measures mainly the canopy of trees in forests. In order to resolve the structure and internal layers of trees / forests, a larger wave length such as L-band seems more suitable as it penetrates vegetation.
  - Finally, a full-polarimetric system would improve the information content and expressiveness of measurements especially over, e.g., vegetation or soil- and moisture.
- 2) *Constraints:* In addition, several new constraints were considered for the acquisition planning.
- The maximal duration of a data take was limited to slow down the degradation of the battery.
  - A reduction of the number of ground stations significantly reduced the contact time per orbit and, thus, the amount of data that can be acquired.
  - Additional margins and a potential replanning of acquisitions needed to be foreseen in the planning to be able to react on delays caused by outages due to satellite ageing.



3) *Acquisitions*: With this input the planning process was executed. An acquisition timeline was derived using the TAP [21]. The resulting acquisitions were started in September 2017 and lasted until June 2020. This is half a year longer than planned due to conflicts with commercial customers over hot spots or high priority sites especially in Europe or over mining areas. In addition, an outage in the SAR instrument on the TanDEM-X satellite in 2019 led to a delay of about two months. Currently, the data are being processed and mosaicked into the change DEM product, which is planned to be completed around 2023.

In total 18 200 change DEM acquisitions have been acquired during the three years acquisition phase. Fig. 12 shows the coverage of the Change DEM acquisition over Europe. The blue acquisitions indicate one single coverage, while cyan, green, or orange indicate two or more acquisitions. An example of a Change DEM is given in Fig. 13. It clearly shows the changes in a mining area in eastern Australia from 2012 to 2018 and underlines the great value of such a globally available product.

### G. Science Phase 2020–2022

The acquisition of the Change DEM coverage was complete in June 2020. With this, TanDEM-X entered into another science phase. Based on the experience and results gained from the continuous science acquisitions and the science phase 2014–2016, the focus of this phase is put on the permafrosted arctic regions [64] and on forested areas. In addition, the largest cities of the world are mapped with different baselines in order to allow 3-D city monitoring [65] and a possible update of the global urban footprint [66]. The designated regions are shown in Fig. 14.

## VI. CONCLUSION

The TanDEM-X mission is a great success both in terms of DEM products for scientific use and as a provider of a commercial global DEM product by the partner Airbus D&S. The mission has been successfully running through different mission phases. Two global DEM products were acquired with the first one being available since 2016 and the second one being processed at the moment. Different scientific phases served the scientific community with a great variety of TanDEM-X products ranging from nominal stripmap and spotlight products to various experimental data takes or acquisitions with very large horizontal or very short along-track baselines over dedicated regions. In total, more than 160 000 interferometric acquisitions have successfully been performed and can be accessed by the users of the system. With its success and this great amount of data TanDEM-X is also a forerunner for future bistatic systems with much higher imaging capabilities like Tandem-L.

## REFERENCES

- [1] G. Krieger *et al.*, “TanDEM-X: A satellite formation for high resolution SAR interferometry,” *IEEE Trans. Geosci. Remote Sens.*, vol. 45, no. 11, pp. 3317–3341, Nov. 2007.
- [2] M. Zink *et al.*, “TanDEM-X: The new global DEM takes shape,” *IEEE Geosci. Remote Sens. Mag.*, vol. 2, no. 2, pp. 8–23, Jun. 2014.
- [3] M. Zink and A. Moreira, “TanDEM-X mission status: The new topography of the earth takes shape,” in *Proc. Int. Geosci. Remote Sens. Symp.*, Canada, 2014, pp. 3386–3389.
- [4] P. Rizzoli *et al.*, “Generation and performance assessment of the global TanDEM-X digital elevation model,” *ISPRS J. Photogrammetry Remote Sens.*, vol. 132, pp. 119–139, 2017. doi: [10.1016/j.isprsjprs.2017.08.008](https://doi.org/10.1016/j.isprsjprs.2017.08.008) ISSN 0924-2716.
- [5] I. Hajnsek *et al.*, “Tandem-X: Mission status and science activities,” in *Proc. IEEE Int. Geosci. Remote Sens. Symp.*, Yokohama, Japan, 2019, pp. 4477–4479.
- [6] G. Krieger *et al.*, “TanDEM-X: A radar interferometer with two formation-flying satellites,” *Acta Astronautica*, vol. 89, pp. 83–98, 2014.
- [7] S. D’Amico and O. Montenbruck, “Proximity operations of formation flying spacecraft using an eccentricity/inclination vector separation,” *J. Guid., Control, Dyn.*, vol. 29, no. 3, pp. 554–563, 2004.
- [8] H. Fiedler and G. Krieger, “Close formation flight of passive receiving micro-satellites,” in *Proc. Int. Symp. Space Flight Dyn.*, Oct. 2004, Paper 1030.
- [9] J. S. Ardaens, S. D’Amico, B. Kazeminejad, O. Montenbruck, and E. Gill, “Spaceborne autonomous and ground based relative orbit control for the TerraSAR-X/TanDEM-X formation,” in *Proc. Int. Symp. Space Flight Dyn.*, 2007, pp. 1–13.
- [10] P. Rizzoli, B. Bräutigam, T. Kraus, M. Martone, G. Krieger, “Relative height error analysis of TanDEM-X elevation data,” *ISPRS J. Photogrammetry Remote Sens.*, vol. 73, pp. 30–38, 2012.
- [11] M. Martone, P. Rizzoli, and G. Krieger, “Volume decorrelation effects in TanDEM-X interferometric SAR data,” *IEEE Geosci. Remote Sens. Lett.*, vol. 13, no. 12, pp. 1812–1816, Dec. 2016.
- [12] T. Fritz, C. Rossi, N. Yague-Martinez, F. Rodriguez Gonzalez, M. Lachaise, and H. Breit, “Interferometric processing of TanDEM-X data,” in *Proc. IEEE Int. Geosci. Remote Sens. Symp.*, 2011, pp. 3518–3521.
- [13] B. Bräutigam, P. Rizzoli, M. Martone, M. Bachmann, and G. Krieger, “InSAR and DEM quality monitoring of TanDEM-X,” in *Proc. IEEE Int. Geosci. Remote Sens. Symp.*, Munich, Germany, 2012, pp. 5570–5573.
- [14] M. Bachmann *et al.*, “TanDEM-X acquisition status and calibration of the interferometric system,” in *Proc. IEEE Int. Geosci. Remote Sens. Symp.*, Munich, Germany, 2012, pp. 1–4.
- [15] H. Hauschildt, S. Mezzasoma, H. L. Moeller, M. Witting, and J. Herrmann, “European data relay system goes global,” in *Proc. IEEE Int. Conf. Space Opt. Syst. Appl.*, 2017, pp. 15–18.
- [16] R. Metzger *et al.*, “The tanDEM-X ground station network,” in *Proc. IEEE Int. Geosci. Remote Sens. Symp.*, 2011, pp. 902–905.
- [17] A. Bojarski *et al.*, “10 Years of TanDEM-X mission: A long-term system overview,” *IEEE J. Sel. Topics Appl. Earth Observ. Remote Sens.*, vol. 14, pp. 2522–2534, 2021.
- [18] F. Stathopoulos *et al.*, “Operational Optimization of the Lithium-ion Batteries of TerraSAR-X/TanDEM-X,” *IEEE J. Sel. Topics Appl. Earth Observ. Remote Sens.*, vol. 14, pp. 3243–3250, 2021, submitted.
- [19] S. Buckreuss *et al.*, “Ten years of TerraSAR-X operations,” *Remote Sens.*, vol. 10, no. 6, pp. 1–28, 2018.
- [20] H. Fiedler, G. Krieger, M. Zink, M. Geyer, and J. Jäger, “The TanDEM-X acquisition timeline and mission plan,” in *Proc. Eur. Conf. Synthetic Aperture Radar*, 2008, pp. 1–4.
- [21] C. J. Ortega-Miguel, D. Schulze, M. D. Polimeni, J. Böer, P. Rizzoli, and M. Bachmann, “TanDEM-X acquisition planner,” in *Proc. Eur. Conf. Synthetic Aperture Radar*, Nuremberg, Germany, 2012, pp. 1–4.
- [22] M. Younis, R. Metzger, and G. Krieger, “Performance prediction of a phase synchronization link for bistatic SAR,” *IEEE Geosci. Remote Sens. Lett.*, vol. 3, no. 3, pp. 429–433, Jul. 2006.
- [23] F. Mrowka *et al.*, “The joint TerraSAR-X /TanDEM-X mission planning system,” in *Proc. IEEE Int. Geosci. Remote Sens. Symp.*, 2011, pp. 3971–3974.
- [24] [Online]. Available: <https://tandemx-science.dlr.de/>, Accessed: Sep. 24, 2020.
- [25] H. Gonzalez *et al.*, “Bistatic system calibration in TanDEM-X to ensure the global digital elevation model quality,” *ISPRS J. Photogrammetry Remote Sens.*, vol. 73, pp. 3–11, 2012.
- [26] T. Kraus, B. Bräutigam, J. Mittermayer, S. Wollstadt, and C. Grigorov, “TerraSAR-X staring spotlight mode optimization and global performance predictions,” *IEEE J. Sel. Topics Appl. Earth Observ. Remote Sens.*, vol. 9, no. 3, pp. 1015–1027, Mar. 2016.
- [27] J. Mittermayer, S. Wollstadt, P. Prats-Iraola, P. Lopez-Dekker, G. Krieger, and A. Moreira, “Bidirectional SAR imaging mode,” *IEEE Trans. Geosci. Remote Sens.*, vol. 51, no. 1, pp. 601–614, Jan. 2013.

- [28] R. Romeiser, S. Suchandt, H. Runge, U. Steinbrecher, and S. Grunler, "First analysis of TerraSAR-X along-track InSAR-derived current fields," *IEEE Trans. Geosci. Remote Sens.*, vol. 48, no. 2, pp. 820–829, Feb. 2010.
- [29] T. Fritz, H. Breit, C. Rossi, U. Balss, M. Lachaise, and U. Duque, "Interferometric processing and products of the TanDEM-X mission," in *Proc. Int. Geosci. Remote Sens. Symp.*, Munich, Germany, 2012, pp. 1904–1907.
- [30] Accessed: Sep. 24, 2020. [Online]. Available: <https://eoweb.dlr.de/egp/>
- [31] M. Bachmann and H. Hofmann, "Challenges of the TanDEM-X Commissioning Phase," in *Proc. Eur. Conf. Synthetic Aperture Radar*, Aachen, Germany, 2010, pp. 1–3.
- [32] M. Schwerdt *et al.*, "In-Orbit calibration of the TanDEM-X system," in *Proc. Int. Geosci. Remote Sens. Symp.*, Vancouver, Canada, Jul. 2011.
- [33] M. Bachmann and H. Hofmann, "TanDEM-X commissioning phase: Execution overview and first results," in *Proc. CEOS SAR Cal/Val Workshop*, Zurich, Switzerland, Sep. 2010.
- [34] M. Bachmann and M. Zink, "The TanDEM-X mission — bi-static SAR for a global DEM," in *Proc. Int. Asia-Pacific Conf. Synthetic Aperture Radar*, 2011, pp. 1–4.
- [35] T. Fritz, H. Breit, C. Rossi, U. Balss, M. Lachaise, and S. Duque, "Interferometric processing and products of the TanDEM-X mission," in *Proc. IEEE Int. Geosci. Remote Sens. Symp.*, 2012, pp. 1904–1907.
- [36] H. Breit, M. Lachaise, U. Balss, C. Rossi, T. Fritz, and A. Niedermeier, "Bistatic and interferometric processing of TanDEM-X data," in *Eur. Conf. Synthetic Aperture Radar*, Nuremberg, Germany, 2012, pp. 93–96.
- [37] M. Bachmann *et al.*, "Calibration of the bistatic TanDEM-X interferometer," in *Proc. Eur. Conf. Synthetic Aperture Radar*, Nuremberg, Germany, 2012, pp. 97–100.
- [38] R. Kahle, B. Schlepp, S. Aida, M. Kirschner, and M. Wermuth, "Flight dynamics operations of the TanDEM-X formation," in *Proc. Int. Conf. Space Operat. (SpaceOps)*, 2012, pp. 1–12, doi: [10.2514/6.2012-1275094](https://doi.org/10.2514/6.2012-1275094).
- [39] M. Lachaise, T. Fritz, U. Balss, R. Bamler, and M. Eineder, "Phase unwrapping correction with dual-baseline data for the TanDEM-X mission," in *Proc. IEEE Int. Geosci. Remote Sens. Symp.*, Munich, Germany, 2012, pp. 5566–5569.
- [40] E. Maurer, R. Kahle, G. Morfill, B. Schlepp, and S. Zimmermann, "Reversal of TanDEM-X's relative motion from counter-clockwise to clockwise," in *Proc. Int. Conf. Space Operat. (SpaceOps)*, 2014, pp. 1–12.
- [41] M. Martone, B. Bräutigam, P. Rizzoli, and G. Krieger, "TanDEM-X performance over sandy areas," in *Proc. Eur. Conf. Synthetic Aperture Radar*, Berlin, Germany, 2014, pp. 1–4.
- [42] T. G. Farr *et al.*, "The shuttle radar topography mission," *Rev. Geophys.*, vol. 45, no. 2, 2007, Art. no. RG2 004.
- [43] B. Schutz, H. Zwally, C. Shuman, D. Hancock, and J. Di Marzio, "Overview of the ICESat mission," *Geophysical Res. Lett.*, vol. 32, no. 21, pp. 1–4, 2005.
- [44] C. Wecklich, C. Gonzalez, and B. Bräutigam, "Height accuracy for the first part of the global TanDEM-X DEM data," in *Proc. Geomorphometry*, Poznan, Poland, 2015.
- [45] P. Rizzoli, B. Bräutigam, T. Kraus, M. Martone, and G. Krieger, "Relative height error analysis of TanDEM-X elevation data," *ISPRS J. Photogrammetry Remote Sens.*, vol. 73, pp. 30–38, 2012.
- [46] C. Gonzalez *et al.*, "The new global digital elevation model: TanDEM-X DEM and its final performance," in *Proc. Eur. Geosciences Union Gen. Assem.*, 2017, p. 1.
- [47] B. Bello, J. L., M. Martone, P. Prats-Iraola, and B. Bräutigam, "First characterization and performance evaluation of bistatic TanDEM-X experimental products," *IEEE J. Sel. Topics Appl. Earth Observ. Remote Sens.*, vol. 9, no. 3, pp. 1058–1071, Mar. 2016.
- [48] A. Elyouncha, L. E. B. Eriksson, R. Romeiser, and L. M. H. Ulander, "Measurements of sea surface currents in the Baltic sea region using Spaceborne along-track InSAR," *IEEE Trans. Geosci. Remote Sens.*, vol. 57, no. 11, pp. 8584–8599, Nov. 2019.
- [49] S. Nghiem *et al.*, "Remote sensing of Antarctic Sea ice with coordinated aircraft and satellite data acquisitions," in *Proc. IEEE Int. Geosci. Remote Sens. Symp.*, Valencia, Spain, 2018, pp. 1–4.
- [50] P. López-Dekker, H. Rott, P. Prats-Iraola, B. Chapron, K. Scipal, and E. D. Witte, "Harmony: An earth explorer 10 mission candidate to observe land, ice, and ocean surface dynamics," in *Proc. IEEE Int. Geosci. Remote Sens. Symp.*, Yokohama, Japan, 2019, pp. 8381–8384.
- [51] T. G. Yitayew, A. P. Doulgeris, T. Eltoft, W. Dierking, C. Brekke, and A. Rösel, "Sea ice segmentation using Tandem-X pursuit monostatic and alternative bistatic modes," in *Proc. IEEE Int. Geosci. Remote Sens. Symp.*, Fort Worth, TX, USA, 2017, pp. 334–337.
- [52] D. Velotto, F. Nunziata, C. Bentes, M. Migliaccio, and S. Lehner, "Investigation of the experimental TanDEM-X pursuit monostatic mode for oil and ship detection," in *Proc. IEEE Int. Geosci. Remote Sens. Symp.*, 2016, pp. 4023–4026.
- [53] P. Lumsdon *et al.*, "An encounter with pursuit monostatic applications of TanDEM-X mission," in *Proc. IEEE Int. Geosci. Remote Sens. Symp.*, 2015, pp. 3187–3190.
- [54] S. Suchandt and H. Runge, "Ocean surface observations using the TanDEM-X satellite formation," *IEEE J. Sel. Topics Appl. Earth Observ. Remote Sens.*, vol. 8, no. 11, pp. 5096–5105, Nov. 2015.
- [55] B. Zhang *et al.*, "Ship detection and velocity estimation in quad polarimetric SAR images from pursuit monostatic mode of TerraSARX and TanDEM-X," in *Proc. IEEE Int. Geosci. Remote Sens. Symp.*, Fort Worth, TX, USA, 2017, pp. 1860–1863.
- [56] J. Bueso-Bello, P. Prats-Iraola, M. Martone, J. Reimann, U. Steinbrecher, and P. Rizzoli, "Performance evaluation of TanDEM-X quad-polarization products in bistatic mode," *IEEE J. Sel. Topics Appl. Earth Observ. Remote Sens.*, vol. 11, no. 3, pp. 787–799, Mar. 2018.
- [57] T. Kraus, G. Krieger, M. Bachmann, and A. Moreira, "Spaceborne demonstration of distributed SAR imaging with TerraSAR-X and TanDEM-X," *IEEE Geosci. Remote Sens. Lett.*, vol. 16, no. 11, pp. 1731–1735, Nov. 2019.
- [58] T. Kraus, B. Bräutigam, M. Bachmann, G. Krieger, and J. Mittermayer, "TerraSAR-X and TanDEM-X: A unique platform to demonstrate the capabilities of distributed SAR satellite systems," in *Proc. ONERA-DLR Aerosp. Symp.*, Oberpfaffenhofen, Germany, 2016, pp. 1–2.
- [59] J. M. Lopez-Sanchez, F. Vicente-Guijalbaa, E. Erten, M. Campos-Taberner, and F. J. Garcia-Haroc, "Retrieval of vegetation height in rice fields using polarimetric SAR interferometry with TanDEM-X data," *Remote Sens. Environ.*, vol. 192, pp. 30–44, Apr. 2017.
- [60] A. Alonso-González, H. Joerg, K. Papathanassiou, and I. Hajnsek, "Dual-polarimetric agricultural change analysis of long baseline TanDEM-X time series data," in *Proc. IEEE Int. Geosci. Remote Sens. Symp.*, Jul. 10–15, 2016.
- [61] B. Wessel *et al.*, "Concept and first example of TanDEM-X high-resolution DEM," in *Proc. Eur. Conf. Synthetic Aperture Radar*, Hamburg, Germany, 2016, pp. 1–4.
- [62] S. Buckreuss, T. Fritz, M. Bachmann, and M. Zink, "TerraSAR-X and TanDEM-X mission status," in *Proc. Eur. Conf. Synthetic Aperture Radar*, 2018, pp. 1–4.
- [63] A. Moreira *et al.*, "Tandem L: A highly innovative bistatic SAR mission for global observation of dynamic processes on the earth's surface," *IEEE Geosci. Remote Sens. Mag.s*, vol. 3, no. 2, pp. 8–23, Jun. 2015.
- [64] S. Zwieback *et al.*, "Monitoring permafrost and thermokarst processes with TanDEM-X DEM time series: Opportunities and limitations," in *Proc. IEEE Int. Geosci. Remote Sens. Symp.*, 2016, pp. 332–335.
- [65] X. X. Zhu, N. Ge, and M. Shahzad, "Joint sparsity in SAR tomography for urban mapping," *IEEE J. Sel. Topics Signal Process.*, vol. 9, no. 8, pp. 1498–1509, Dec. 2015.
- [66] T. Esch *et al.*, "Urban footprint processor – fully automated processing chain generating settlement masks from global data of the TanDEM-X mission," *IEEE Geosci. Remote Sens. Lett.*, vol. 10, no. 6, pp. 1617–1621, Nov. 2013.



**Markus Bachmann** received the Dipl.-Ing. and Ph.D. degrees in electrical engineering from the Technical University of Karlsruhe, Karlsruhe, Germany, in 2005 and 2015, respectively.

In 2005, he was with the Microwaves and Radar Institute, German Aerospace Center. From 2005 to 2011, he was in-charge of the implementation and calibration of the TerraSAR-X/TanDEM-X antenna model. From 2006 to 2010, he assessed the potentials and methods of the DEM calibration for TanDEM-X. From 2008 to 2010, he was responsible for the planning and execution of the TanDEM-X commissioning phase. In 2011 and 2012, he performed the interferometric and radiometric calibration of the TanDEM-X system and established the monitoring of the global coverage for the TanDEM-X mission. He has been the Ground Segment Project Manager of the Tandem-L/Rose-L Tandem project since 2016. Since 2012, he has been the head of the Mission Engineering group, which is in-charge of the operational planning of the acquisitions for TanDEM-X and the future missions like Tandem-L, Rose-L Tandem, or HRWS as well as for the analysis of mission relevant aspects in the frame of various SAR missions.



**Thomas Kraus** received the M.Sc. degree in electrical engineering from the University of Ulm, Ulm, Germany, in 2009.

In 2010, he was with the Microwaves and Radar Institute, German Aerospace Center, Oberpfaffenhofen, Germany, where he is currently working in the field of spaceborne SAR. He is involved in the instrument commanding, the processing, and the analysis of scientific and experimental acquisitions in the framework of the projects TerraSAR-X and TanDEM-X. He was responsible for the performance analysis during

the operational implementation of the Staring Spotlight and the wide ScanSAR modes of TerraSAR-X as well as the dual receive antenna mode in the bistatic science phase of TanDEM-X. For the geostationary mission proposal Hydroterra he also contributed the SAR performance analysis. His research interests include radar system performance, the development of innovative SAR modes, and the analysis of distributed satellite SAR systems.



**Allan Bojarski** received the Dipl. -Ing. degree in aerospace engineering from the Technical University of Munich, Munich, Germany, in 2014.

After two years performing battery simulations for the Daimler R&D Department, Ulm, Germany, in 2016, he was with the Microwaves and Radar Institute, German Aerospace Center, Oberpfaffenhofen, Germany. He is currently involved in various spaceborne SAR projects as a mission engineer. In this context, he is responsible for the long-term system monitoring of TerraSAR-X/TanDEM-X satellites and

the scientific acquisition planning for the TanDEM-X mission. Furthermore, he is designing mission scenarios, SAR satellite formations and observation concepts for several SAR missions such as Tandem-L or HRWS.



**Maximilian Schandri** received the B.Sc. and M.Sc. degrees in physics from the University of Erlangen–Nuremberg, Erlangen, Germany, in 2016 and 2018, respectively.

Since 2018, he has been a scientific employee with the Microwaves and Radar Institute, German Aerospace Center, Oberpfaffenhofen, Germany, where he is involved in the acquisition planning of the TanDEM-X mission. He also contributed to a software for calculating the performance of a SAR system concept with a geosynchronous orbit.



**Johannes Böer** received the Diploma degree in electrical engineering from Karlsruhe Institute of Technology, Karlsruhe, Germany, in 2004.

During his studies, he was involved in the development of external calibration hardware (ground receiver/transponder) for the TerraSAR-X satellite. Since 2004, he has been with the Microwaves and Radar Institute, German Aerospace Center, Wessling, Germany, working in the System Engineering and Calibration segment of TerraSAR-X and, later, TanDEM-X. He has been supported the successful

commissioning of the SAR instrument of TerraSAR-X and, since 2017, is leading the System Engineering and Calibration Segment of TerraSAR-X and TanDEM-X.



**Thomas Edmund Busche** received the Diploma degree in geography from Georg-August-University, Göttingen, Germany, in 2000.

From 2000 to 2002, he was with the private sector, involved in the field of remote sensing and the Geographic Information System. From 2003 to 2007, he was a Research Assistant with the Alfred Wegener Institute for Polar and Marine Research, Bremerhaven, Germany, and the Sea Ice Physics working group. Since 2007, he has been with the German Aerospace Center (DLR), Microwaves and Radar Institute, and

the Polarimetric Interferometry working group, Oberpfaffenhofen, Germany. He is currently involved in all aspects of science coordination activities of DLR's TanDEM-X mission.



**José-Luis Bueso-Bello** received the Ingeniero degree in telecommunications engineering from the Universidad Politécnica de Valencia, Valencia, Spain, in 2003, and the M. Sc. degree in earth oriented space science and technology from the Technische Universität München, Munich, Germany, in 2007.

In 2003, he was with the Microwaves and Radar Institute, German Aerospace Center (DLR), Oberpfaffenhofen, Germany, as System Engineer with the Department of Reconnaissance and Security, where he worked in the definition, design, and mission analysis for different SAR projects.

In 2010, he was with the Satellite SAR Systems Department, where he is currently working as a Project Engineer with main focus on the plan, evaluation, and performance monitoring of the TanDEM-X SAR acquisitions and their image quality assessment. His main research interests include signal processing, earth system monitoring, and artificial intelligence algorithms applied to SAR images.



**Christo Grigorov** received the M.Sc. degree in computer science from the Technical University Sofia, Sofia, Bulgaria, in 2005, and the double M.Sc. degree in space science and technology from the Julius-Maximilians University of Würzburg, Würzburg, Germany and from the Lulea University of Technology, Lulea, Sweden, in 2007.

In 2008, he was with the Microwaves and Radar Institute (HR), German Aerospace Center (DLR), Germany. He has been working as Systems Engineer and Software Engineer for ground segments of radar

satellite missions such as TerraSAR-X and TanDEM-X with focus on system design, integration, and implementation of new features. He leads the Systems Engineering team with HR, DLR.

Mr. Grigorov has been a member of the International Council on Systems Engineering since 2009 and a holder of the INCOSE Associate Systems Engineering Professional Certificate.



**Ulrich Steinbrecher** received the Dipl.-Ing. degree in electrical engineering/communication from the University of Siegen, Siegen, Germany, in 1990.

In 1990, he started his career with the German Aerospace Center, Wessling, Germany, with the development of a SAR raw data simulator. Then, he was in software development with the X-SAR Processor and with the joint U.S.–Italian–German SIR-C/XSAR Missions in 1994. When the data were in-house, he concentrated on aspects of the operational SAR processing of high data volumes. In 1995, he

pioneered a completely automatic SAR processing system based on a robot-maintained mass memory archive. Before he became responsible for the development of the raw data analysis and screening system for the shuttle radar topography mission, he developed the software for a phase-preserving ScanSAR processor for Radarsat-1. In the time between the SRTM mission and the start of the TerraSAR-X project, he left the SAR domain for two years and contributed to the SCIAMACHY LIMB processing system. Since 2002, he has been concerned with the TerraSAR-X radar system, and since the launch of the satellite, in 2007, he was responsible for TerraSAR-X instrument operations.





**Stefan Buckreuss** received the Dipl.-Ing. degree in electronics from the Technical University of Munich, Munich, Germany, in 1988 and the Dr.-Ing. degree in aerospace engineering and geodesy from the University of Stuttgart, Stuttgart, Germany, in 1994.

He has been with the Deutsches Zentrum für Luft- und Raumfahrt (DLR), Microwaves and Radar Institute, Oberpfaffenhofen, Germany, since 1988, where he gained broad experience in SAR signal processing, motion compensation, antijamming, and interferometry. Since 2002, he has been engaged with the

German TerraSAR-X/TanDEM-X mission, where he was responsible for the development of the instrument operations and calibration segment until he was assigned the role of the ground segment integration manager. He is currently the TerraSAR-X and TanDEM-X mission manager responsible for the general mission aspects.



**Manfred Zink** received the Dipl.-Ing. degree in physics from the Technical University of Graz, Graz, Austria, in 1987, and the Dr.-Ing. degree in aerospace engineering and geodesy from the University of Stuttgart, Stuttgart, Germany, in 1993.

In 1988, he was with the Microwave and Radar Institute, German Aerospace Center (DLR). He has pioneered the calibration techniques for both air- and spaceborne SAR sensors. He was the Lead X-SAR Calibration Engineer for both SIR-C/X-SAR missions in 1994 and for the SRTM mission in 2000.

In August 2000, he was with the European Space Agency and took over the responsibility for the calibration/validation of the ASAR onboard ENVISAT. After successful in-orbit commissioning of the ASAR, he was appointed as the Principal System Engineer for ESA's TerraSAR-L Program. In May 2005, he returned to DLR's Microwaves and Radar Institute, where he is currently heading the Satellite SAR Systems Department. From 2006 to 2015, he was leading the TanDEM-X ground segment project.

Dr. Zink has been an active member of the CEOS Working Group on Calibration and Validation, SAR Subgroup, since 1991, and from 2011 to 2016, he has been chairing this group. He was the recipient of the DLR Science Award in 1991 and the EUSAR Best Paper Award in 2008. In 2012, he and his colleagues were presented with the IEEE W.R.G. Baker Prize Paper Award and have been nominated for the German Federal President's Prize for Technology and Innovation. He was the general chairman of the European SAR conference 2014.



**Gerhard Krieger** (Fellow, IEEE) received the Dipl.-Ing. (M.S.) and Dr.-Ing. (Ph.D.) (hons.) degrees in electrical and communication engineering from the Technical University of Munich, Munich, Germany, in 1992 and 1999, respectively.

From 1992 to 1999, he was with the Ludwig Maximilians University, Munich, where he conducted multidisciplinary research on neuronal modeling and nonlinear information processing in biological and technical vision systems. Since 1999, he has been with the Microwaves and Radar Institute of the German

Aerospace Center (DLR), Oberpfaffenhofen, Germany, where he started as a Research Associate developing signal processing algorithms for a novel forward-looking radar system employing digital beamforming on receive. From 2001 to 2007, he led the New SAR Missions Group, which pioneered the development of advanced bistatic and multistatic radar systems, such as TanDEM-X, as well as innovative multichannel SAR techniques and algorithms for high-resolution wide-swath SAR imaging. Since 2008, he has been the Head of the Radar Concepts Department which hosts about 40 scientists focusing on new SAR techniques, missions and applications. He has moreover been serving as Mission Engineer with TanDEM-X and he made also major contributions to the development of the Tandem-L mission concept, where he led the Phase-0 and Phase-A studies. Since 2019, he has been moreover a Professor with the Friedrich-Alexander-University Erlangen, Germany. He has authored or coauthored more than 100 peer-reviewed journal papers, 9 invited book chapters, more than 400 conference papers, and more than 20 patents.

Prof. Krieger has been an Associate Editor for the IEEE TRANSACTIONS ON GEOSCIENCE AND REMOTE SENSING since 2012. In 2014, he was the Technical Program Chair for the European Conference on Synthetic Aperture Radar and as a Guest Editor for the IEEE JOURNAL OF SELECTED TOPICS IN APPLIED EARTH OBSERVATIONS AND REMOTE SENSING. He was the recipient of the several national and international awards, including two best paper awards at the European Conference on Synthetic Aperture Radar, two transactions prize paper awards of the IEEE Geoscience and Remote Sensing Society, and the W.R.G. Baker Prize Paper Award from the IEEE Board of Directors.